ORIGINAL ARTICLE

Oleamide–PDMS copolymer for coating urinary catheters with anti-adhesive and anti-biofilm properties

Jiwon Park[1] · Eunseok Seo[2] · Yang-Hoon Kim[1] · Ji-Young Ahn[1] · Da Hyeon Choi[1] · Kyeong Eun Lee[1] · Yoon Shin Park[1]

Abstract

Background Biofilm formation on biomedical devices is a prevalent problem that can result in several complications and is responsible for over 80% of all clinical infections. Successful treatment of biofilms requires a 1500-fold increase in antibiotic concentration, which can lead to toxicity and antibiotic resistance. Therefore, biofilm growth and infection in biomedical devices are significant concerns, and their prevention is a crucial medical challenge.

Objectives To prevent biofilm infection by modifying the surface properties of medical devices, an oleamide–polydimethyl-siloxane (PDMS) copolymer was synthesized to demonstrate anti-adhesion to bacteria and anti-biofilm activity. Catheter coatings for biomedical device applications were evaluated by blood toxicity.

Results We synthesized an oleamide–PDMS copolymer (OPC) and evaluated its anti-adhesion and anti-biofilm activities against the gram-negative bacterium *Escherichia coli* (*E. coli*) and the gram-positive bacterium *Staphylococcus aureus* (*S. aureus*). The OPC films inhibited the growth of biofilms by inhibiting early adhesion of bacteria. As the oleamide content increased, the ability of the OPC films to inhibit *E. coli* and *S. aureus* surface adhesion also increased. In addition, the biofilm formation ability of both *E. coli* and *S. aureus* was significantly inhibited at oleamide contents of 2.5 wt% and 5 wt% in the OPC films, respectively. OPC films were applied to the catheter using a simple dip-coating method, and a low hemolytic capacity was confirmed by hemolysis analysis.

Conclusion The anti-adhesion ability of OPC enables them to prevent biofilm growth and infection. Furthermore, they can be applied in medical devices owing to their high biocompatibility and poor hemolytic properties.

Keywords Oleamide · PDMS · Anti-adhesive · Anti-biofilm · Catheter

Introduction

Biofilms are composed of extracellular polymeric substances, such as proteins/enzymes, exopolysaccharides, lipids, and DNA/RNA, that are secreted by microbes. Biofilm growth on biomedical devices is a widespread problem that can result in infection and other complications (Khatoon et al. 2018). At least 80% of all clinical infections in the human body are associated with biofilms that form on various biological surfaces or medical devices (Römling and Balsalobre 2012). It has been reported that biofilms require 1,500 times more antibiotic concentration than planktonic

✉ Yoon Shin Park
pys@cbnu.ac.kr

Jiwon Park
jiwon79@chungbuk.ac.kr

Eunseok Seo
seven@sogang.ac.kr

Yang-Hoon Kim
kyh@chungbuk.ac.kr

Ji-Young Ahn
jyahn@chungbuk.ac.kr

Da Hyeon Choi
dahyeon@chungbuk.ac.kr

Kyeong Eun Lee
dlruddms1223@chungbuk.ac.kr

1 Department of Biological Sciences and Biotechnology, School of Biological Sciences, College of Natural Sciences, Chungbuk National University, Cheongju 28644, Republic of Korea

2 Department of Mechanical Engineering, Sogang University, Seoul 04107, Republic of Korea

bacteria, which raises concerns regarding toxicity and antibiotic resistance (Tenke et al. 2006). Therefore, the treatment of diseases caused by biofilms is aggressive and consists of the removal of implanted medical devices, surgical removal of necrotic tissue, or the administration of strict antibiotic combination therapy (Del Pozo 2018).

In many medical applications, implant infections lead to the formation of biofilms during implantation procedures or long-term implant use after surgery. The increased use of biomedical devices, such as implants, catheter, and prostheses, can increase the risk of various types of infection (Dudeck et al. 2013). Infections including catheter-associated urinary tract infections (CAUTIs) are among the most common types of healthcare-associated infections and are particularly dangerous in patients with long-term indwelling catheters (Nicolle 2014). Other infections include central line-associated bloodstream infections (CLABIs), which poses a high risk of bloodstream infections (Lutufyo et al. 2022), High-risk ventilator-associated pneumonia (VAP) in patients requiring mechanical ventilation (Baidya et al. 2021), surgical site infections (SSIs) (Hrynyshyn et al. 2022), hospital-acquired pneumonia (Assefa and Amare 2022), and dental implants (Larsen and Fiehn 2017) have all been major causes of hospital-acquired or healthcare-associated infections.

Various strategies have been developed to prevent biofilm formation and to degrade established biofilms. Biofilm degradation can be used to kill bacteria or disrupt biofilm formation using physical or chemical treatments (Liu et al. 2022), as well as light-based treatments such as photodynamic therapy (PDT) (Hu et al. 2018) or ultraviolet (UV) light (Torkzadeh et al. 2021). Additionally, it is possible to reduce bacterial adhesion and biofilm formation by altering the surface characteristics of biomedical devices. Antibiotics are commonly used to prevent biofilm formation on biomaterial surfaces. Antibiotic molecules are directly bound to the biomaterial surface at the molecular level, packaged in nanoparticles (Ramasamy and Lee 2016) or microcapsules, (Mechmechani et al. 2022) and applied to the biomaterial surface for release. Methods involving the slow release of antibiotics may be more effective than the use of antibiotics immobilized on surfaces because the required concentration of antibiotics can be regulated by varying the type and rate of release. However, the antibiotic resistance of biofilms requires the use of high concentrations of antibiotics (Trubenová et al. 2022), and the dead microbes can cover the antibiotic surface and consequently lose their antibacterial properties.

The use of an anti-adhesion coating on the surface of medical devices to prevent the attachment of pathogenic bacteria is a successful method for preventing infections via indwelling medical devices (Rodrigues 2011). It is possible to change the surface modification of a medical device by coating without altering its bulk properties. The physicochemical properties of medical device surfaces, such as the introduction of specific chemical functional groups (Harding and Reynolds 2014), surface roughness, surface charge, and surface wettability (Desrousseaux et al. 2013), significantly affect the number of attached bacteria and the extent of their growth and spread. Such surface modifications can prevent bacterial adhesion and biofilm formation on material surfaces, improve biocompatibility, and reduce the risk of infection (Quinn et al. 2020).

Oleamide is a naturally occurring primary fatty acid that induces sleep by interacting with multiple neurotransmitter systems (Huitrón-Reséndiz et al. 2001). Synthetic oleamides are used in several industrial applications such as slip agents, lubricants, and corrosion inhibitors (Getachew et al. 2016). In a preliminary study (Seo et al. 2020), the effectiveness of inhibiting the attachment of algal spores and mussels was investigated by creating an eco-friendly oleamide–polydimethylsiloxane (PDMS) copolymer (OPC) for sustainable prevention of biofouling and efficient drug reduction. In marine environments, studies on fatty acid amide-based oleogels have revealed a range of effects, including reduced drag, anti-biofouling, and anti-icing (Getachew et al. 2016).

In this study, we synthesized an oleamide–PDMS copolymer and evaluated its anti-adhesion and anti-biofilm activity against the gram-negative bacteria *Escherichia coli* (*E. coli*) and the gram-positive bacterium *Staphylococcus aureus* (*S. aureus*), as a catheter coating for biomedical device applications, and its blood toxicity. To the best of our knowledge, this is the first study to explore the potential of oleamide as an antibacterial coating for biomedical devices. Our findings provide a basis for improving the overall effectiveness of biomedical devices in the medical environment by exploiting the ability of oleamide to prevent the attachment of pathogenic bacteria, thereby preventing infections via indwelling medical devices.

Materials and methods

Fabrication of oleamide–PDMS copolymer and catheter coating

A mixture of the PDMS prepolymer and curing agent was prepared at a weight ratio of 10:1, according to a previous study (Seo et al. 2020). Oleamide powder was prepared at different weight percentages (0.0625–5 wt%) for 10 g of the PDMS mixture. The oleamide powder was completely dissolved in toluene under sonication at 70 °C for 2 h. Then, the oleamide solution was quickly added to PDMS solution and mixed.

Foley urinary catheters (22 Fr) (Sewon Medical, Seoul, Korea) were cut into 1 cm fragments. These fragmented

catheters were dipped into solutions of the PDMS mixture and then dried at 70 °C for 24 h.

Bacterial culture

E. coli (KCTC1682, a gram-negative bacterium) and *S. aureus* (KCCM40881, a gram-positive bacterium) were obtained from the Korean Collection for Type Cultures (Daejeon, Korea). These bacteria in lysogeny broth were cultured at 37 °C in a cultured incubator. A single colony formed on the LB agar plate was inoculated and cultured in liquid medium to prepare bacteria at a concentration of 5×10^6 colony-forming units (CFU)/mL.

Sample surface characterization

The contact angle (CA) was measured to evaluate the wetting properties of the fabricated OPC surfaces. The static CA of a 3-µL water droplet was measured using a PHOENIX-300 TOUCH (Surface Electro Optics, Suwon, South Korea) to analyze the wettability of the fabricated OPC surfaces. Each sample was measured five times, and the average CA value was calculated.

Field-emission scanning electron microscopy (FE-SEM) images of the sample surfaces were collected using a Zeiss Ultra Plus field-emission scanning electron microscope (ULTRA plus FESEM, Zeiss, Germany) at 3 kV to evaluate the morphology of the samples.

Time-of-flight secondary ion mass spectrometry (ToF-SIMS) measurements were performed to evaluate the chemical components of the OPC-coated surface using an M6 instrument (ION-TOF GmbH, Münster, Germany) with a pulsed 30 keV Bi_3^+ primary ion beam in the spectrometry mode for positive ions. An electron flood gun was used for charge compensation. The positive ion spectra were internally mass-calibrated using the CH_3^+, $C_2H_3^+$, $C_3H_5^+$, and $C_4H_7^+$ peaks.

Anti-adhesion and anti-biofilm assay

The OPC mixture was coated onto a 24-well plate and covered with slip glass (Diameter 12 mm) and then cured at 70 °C for 24 h. The OPC plates were rinsed with phosphate-buffered saline (PBS) to remove the culture broth. *E. coli* and *S. aureus* biofilms were prepared in 24-well microtiter plates using OPC plates. Briefly, 1 mL of the bacterial culture (5×10^6 CFU/mL) was seeded in each well of a 24-well plate and incubated at 37 °C for 17 h. After incubation, the medium was removed, and the wells were washed twice with 1 mL of PBS. To determine the amount of bacterial adhesion and cell viability on the OPC-coated surface, the LIVE/DEAD BacLight Bacterial Viability Kit L-7012 was used for microscopy and quantitative assays (Molecular Probes, Eugene, OR, USA), containing separate

vials of the two-component dyes (SYTO 9 and propidium iodide in a 1:1 mixture) in solution. The excitation/emission maxima of these dyes were FITC for SYTO 9 staining and Texas Red for the propidium iodide staining. For fluorescence imaging of stained cells, confocal laser scanning microscopy (CLSM) was performed using Airyscan technology for super-resolution microscopy (LSM 880; Zeiss, Jena, Germany). Simultaneous dual-channel imaging was used to visualize green and red fluorescence.

The biofilm assay was performed as previously described (D'Almeida et al. 2017). Briefly, 1 mL (5×10^6 CFU/mL) of the bacterial culture was seeded in a 24-well OPC-coated plate and incubated at 37 °C for 72 h. After incubation, the biofilms were washed twice with 1 mL PBS. After removing planktonic cells from the wells, the biofilms were fixed with 99% methanol. The biofilms were stained with 200 µL of 0.5% crystal violet (CV) prepared from a 1% crystal violet solution (Sigma-Aldrich, MD, USA) diluted with distilled water (DW) (Kragh et al. 2019). After 15 min of incubation at room temperature, the unbound CV was removed and washed twice with DW. CV bound to the biofilm in each well was solubilized with 200 µL of 99% ethanol. After 30 min of incubation, 100 µL of the solution was transferred into a 96-well plate. Finally, the absorbance of the CV ethanol solution at 540 nm was determined using a Synergy HTX multi-mode microtiter plate reader (Bio-Tek, Winooski, VT, USA).

Hemolysis

The hemocompatibility of the OPC-coated urinary catheter was assessed using a hemolysis assay (Srisang and Nasongkla 2019; Greco et al. 2020). The red blood cells (RBCs) from defibrinated sheep blood (Kisan Bio Co., Seoul, Korea) were isolated by centrifugation at 3000 rpm for 10 min. RBCs were washed twice with PBS and diluted to 4% with PBS. Each microcentrifuge tube containing the coated catheter was filled with 750 µL of the diluted suspension. As a positive control, 2% Triton X-100 (Sigma-Aldrich) was used, and 20 mM PBS served as the negative control. The tubes were incubated in a shaking incubator at 37 °C at 300 rpm speed for 5 h. After incubation, the RBC suspension was centrifuged at 3000 rpm for 3 min. Then, 100 µL of the supernatant was transferred to 96-well plates, and the absorbance was measured at 576 nm using a Synergy HTX multi-mode reader (Bio-Tek, Winooski, VT)(Ding et al. 2012; Ishiguro et al. 2020). The percentage of hemolysis was calculated using the following equation:

$$\%\text{Hemolysis} = \left(\frac{\text{Abs}_{catheter} - \text{Abs}_{negative}}{\text{Abs}_{positive} - \text{Abs}_{negative}} \right) \times 100,$$

where $\text{Abs}_{catheter}$, $\text{Abs}_{negative}$, and $\text{Abs}_{positive}$ correspond to the absorbance values recorded at 576 nm for different catheter

samples, positive control (Triton X-100), and negative control (DPBS), respectively.

Results

### Characterization of surface chemicals

To analyze the chemical and physical properties of the OPC surface, the water contact angle was used to calculate the surface wetting characteristics, whereas TOF-SIMS analysis was used to investigate the chemical composition of the OPC surface. Figure 1A shows the wettability of the OPC coating film for oleamide concentrations of 0 wt%, 0.625, 1.25, 2.5, and 5 wt%. With the addition of oleamide, the water contact angle and hydrophobicity of the OPC film decreased, and sticky and slippery surfaces were produced as the oleamide content of the OPC film increased.

As the OPC content increased, TOF-SIMS analysis showed an increase in the intensity of the characteristic oleamide molecular secondary ion, $C_{18}H_{35}NO^+$ ($[M+H]^+$) at m/z 282.30, on the OPC surface in the TOF-SIMS positive spectrum (Fig. 1B). In the TOF-SIMS images of the oleamide-specific molecules, the image intensity increased as the oleamide content increased in the OPC films.

Anti-adhesion properties of the OPC films

After 24 h of bacterial growth, the pure PDMS and OPCs coatings with various oleamide contents were analyzed using FE-SEM and LIVE/DEAD staining. Numerous *E. coli* and *S. aureus* cells attached to the PDMS surface; however, bacterial attachment was hindered by the addition of oleamide.

FE-SEM and CLSM images of the surfaces of PDMS and OPC cultured with gram-negative *E. coli* for 24 h are shown in Fig. 2. On the PDMS and 0.625 wt% OPC surfaces, *E. coli* formed biofilms to a comparable degree. Non-uniform biofilm aggregation was observed due to the non-uniform oleamide lubricating layer formed on OPC surface as only a small volume of oleamide was added to pure PDMS. Furthermore, as the contents of oleamide increased to 1.25 wt%, 2.5 wt%, and 5 wt%, the amount of biofilm attached to the substrate decreased. *S. aureus* tended to adhere to the bacteria even at 2.5 wt% OPC, which is a higher concentration than that of *E. coli* and appeared to be uniformly dispersed and adhered to the surface. *E. coli* showed a reduced amount from 1.25 wt% OPC; whereas, *S. aureus* showed adherence even at a higher content (2.5 wt% OPC) and was uniformly dispersed on the surface. In contrast to the OPC-containing oleamide, the biofilm in PDMS forms a thick and compact aggregate. According to confocal images of *E. coli* and *S.*
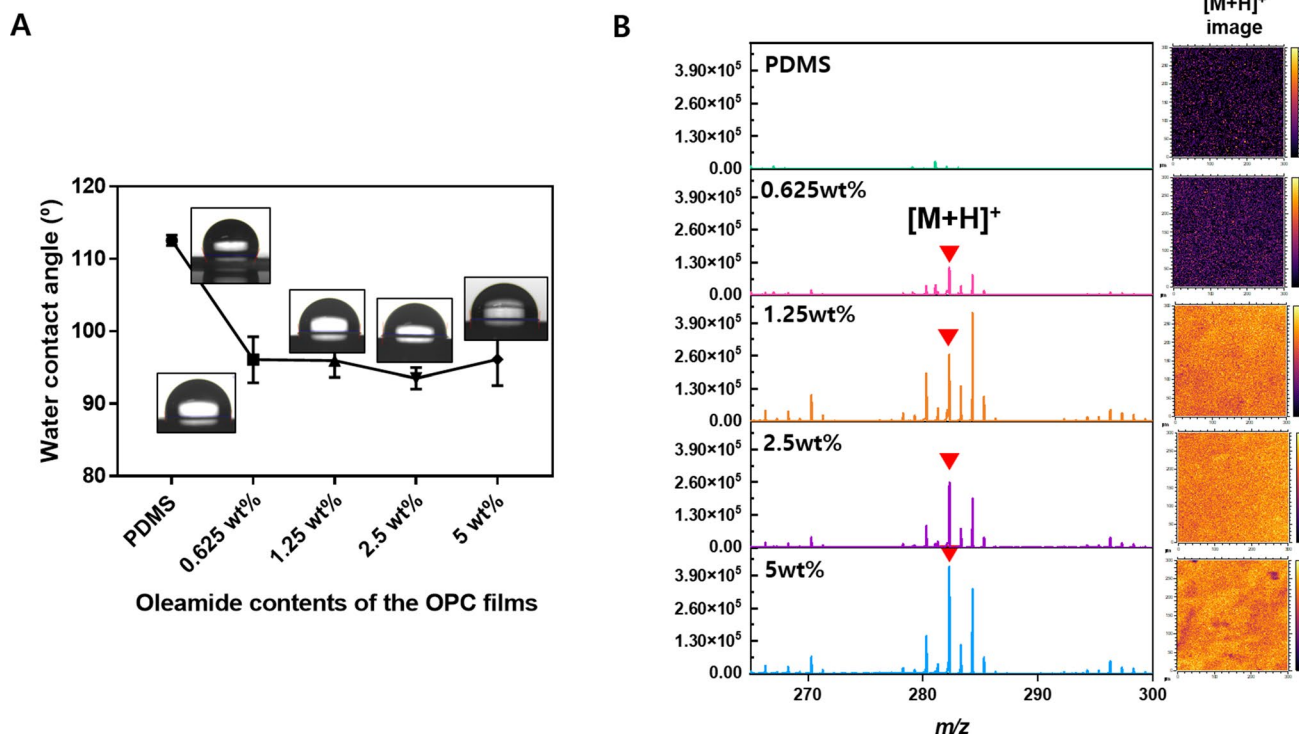
Fig. 1 **A** Contact angle (CA) of the OPC films fabricated with various oleamide contents. The CA of each sample was measured five times, from which the average CA value was calculated. **B** TOF-SIMS positive spectrum and ionic imaging of fabricated OPC with various oleamide contents. Oleamide characteristic molecular secondary ion, $C_{18}H_{35}NO^+$ ($[M+H]^+$), at m/z 282.30
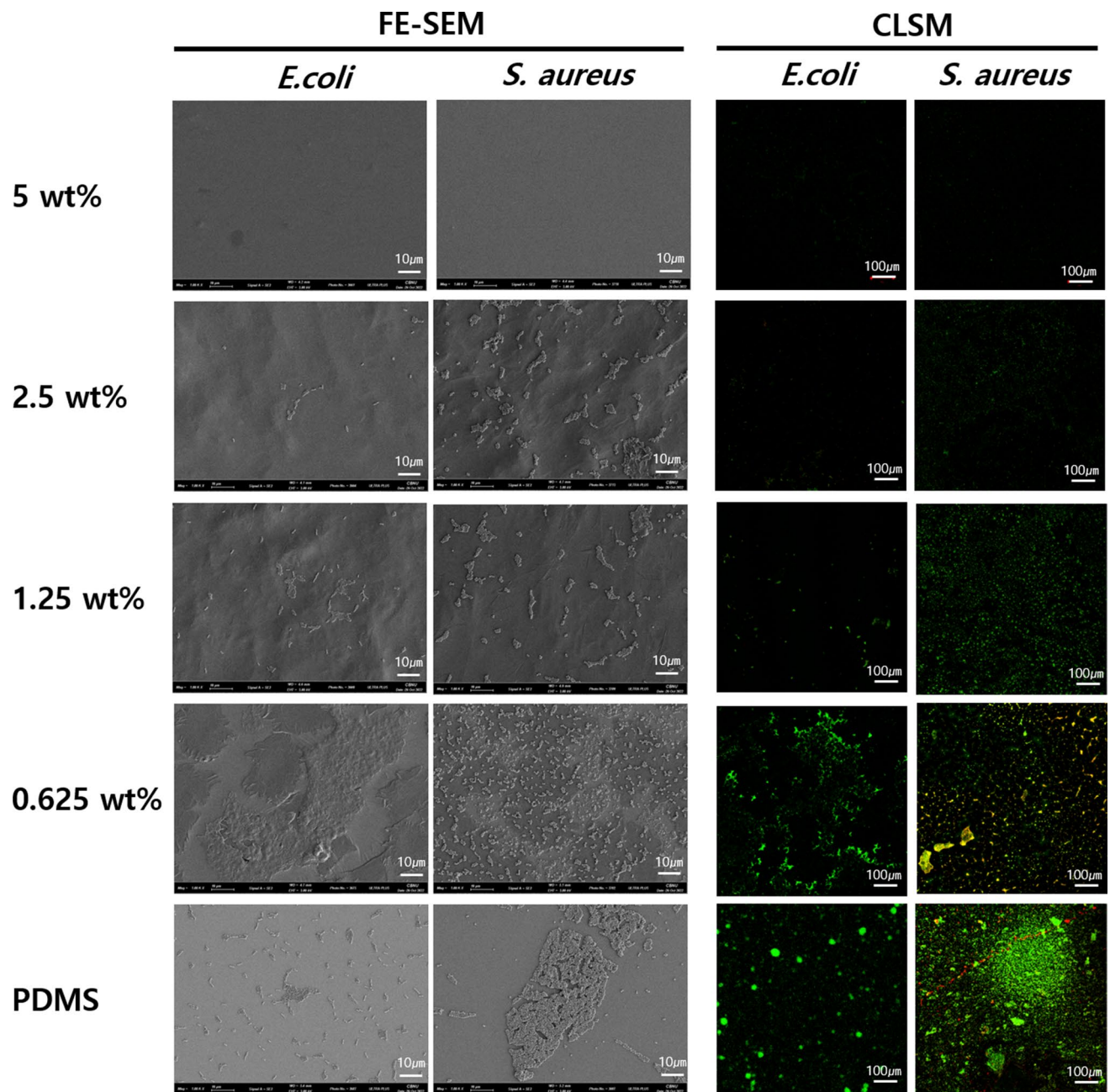
Fig. 2 FE-SEM (Left panel, 1000×magnification) and CLSM (Right panel, 10×magnification) of gram-negative *E. coli* and gram-positive *S. aureus* on OPC coatings: 5 wt%, 2.5 wt%, 1.25 wt%, and 0.625 wt% oleamide of OPC, and pure PDMS. FE-SEM scale bar = 10 μm, fluorescence scale bar = 100 μm. Fluorescence images of the same samples at 488 nm (green) for the SYTO9 signal and 561 nm (red) for the PI signal were merged. The green and red colors represent the viable bacteria and the dead cells, respectively

aureus, although bacterial adhesion was inhibited on the OPC surface during the 24-h incubation period, no bacterial killing effect was observed.

Anti-biofilm properties of the OPC films

Mature biofilms grown for 72 h in 24-well OPC-coated plates were evaluated using a crystal violet biofilm assay.

Biofilm development was significantly inhibited at oleamide content of 2.5 wt% and 5 wt% in the OPC films for both *E. coli* (Fig. 3A) and *S. aureus* (Fig. 3B). Compared with PDMS, biofilm formation was suppressed by 55.37% ($P = 0.035$) and 60.95% ($P = 0.019$) at 2.5% and 5 wt%, respectively, for *E. coli*, and by 72.27% ($P < 0.001$) and 90.92% ($P < 0.0001$) at 2.5% and 5 wt%, respectively, for *S. aureus*.
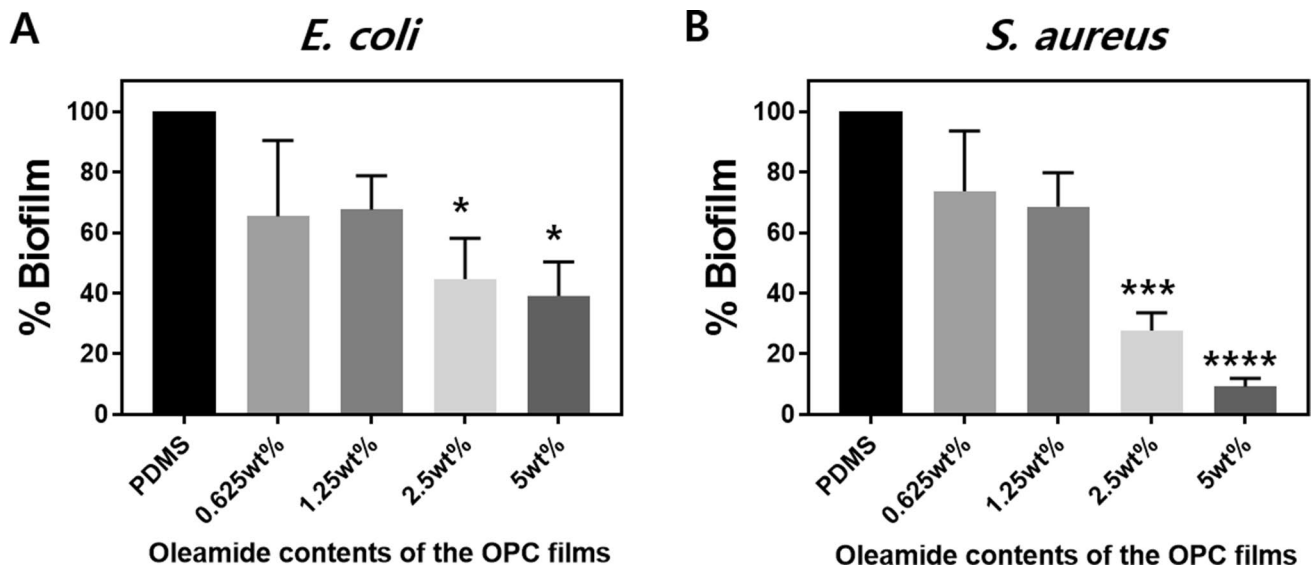
A *E. coli*

B *S. aureus*

Fig. 3 Assessment of mature biofilm biomass for 72 h of incubation by crystal violet staining. Quantification of biofilm formation by crystal violet staining of two bacteria: (**A**) *E. coli* and (**B**) *S. aureus*. The data were obtained from three independent experiments and analyzed by one-way ANOVA (Dunnett T3). (*$P < 0.05$, **$P < 0.01$, ***$P < 0.001$, ****$P < 0.0001$) Graphs show the mean ± standard deviation

Antimicrobial coatings for urinary catheters

The catheters were sliced each 1 cm and soaked in different OPC solutions (Fig. 4A). According to the FE-SEM results of the cross section of the OPC coating film applied to the catheter, the surface coatings had an average thickness of 5 μm (Fig. 4B). Thus, the formation of a sufficient catheter coating using the simple dip-coating process was confirmed. Next, the hemolytic activity of a catheter coated with an OPC film containing varying amounts of oleamide was evaluated using sheep blood (Fig. 4C). The hemolytic index results of PDMS-coated catheters without oleamide and OPC-coated catheters with an oleamide content of 0.625 wt%, 1.25 wt%, 2.5 wt%, and 5 wt% were 2.14 ± 0.61, 1.35 ± 0.16, 1.68 ± 0.16, 1.81 ± 0.37, and 1.49 ± 0.16, respectively (Fig. 4D). The PDMS-coated catheters showed a hemolytic activity of less than 2% for the catheters coated with OPC at all concentrations.

Discussion

The double bond in oleamide induces a hydrosilylation reaction with the silicon hydride of PDMS, resulting in the formation of an OPC coating film (Seo et al. 2020). The TOF-SIMS results indicated that as the oleamide content in the OPC synthesis increased, the number of oleamide molecules on the surface increased, leading to the formation of a slippery surface. Although PDMS is a relatively hard and water-repellent material, its molecular size is small, and it has a flexible chain, allowing it to move easily. It also has a low friction coefficient and a low melting point (Briscoe et al. 1972; Getachew et al. 2016). Consequently, oleamide easily migrates to the outer surface, forming a gliding layer that renders the contact surface slippery. Therefore, oleamide increases the smoothness of the coating film and facilitates bacterial separation. This PDMS-based coating film containing oleamide can exert various surface properties, including biofouling prevention, and can be applied to a variety of medical devices for surface modification without altering the bulk properties of the medical devices.

SEM and CLSM images showed that an increase in the oleamide content of the OPC coating inhibited the bacterial surface attachment ability of both *E. coli* and *S. aureus*. An increase in the number of oleamide molecules on the surface increased the slipperiness of the coating film, which prevented the bacteria from adhering to it. According to the CLSM images, the number of dead bacteria among the attached bacteria was low, and oleamide did not seem to have a bactericidal effect. However, in Fig. 2, *S. aureus* cell death appears to be induced by 0.625 wt% OPC. Nevertheless, because cell death was not observed at a higher oleamide concentration on 1.25wt% OPC, it was difficult to determine whether the OPC coating had an antibacterial effect. Therefore, we anticipate that the anti-biofilm properties of the PDMS-based OPC coating film containing oleamide are due to its ability to inhibit bacterial surface adhesion rather than its antibacterial effect.

Modifying surface properties is an effective way to inhibit bacterial attachment. In particular, the number of bacteria
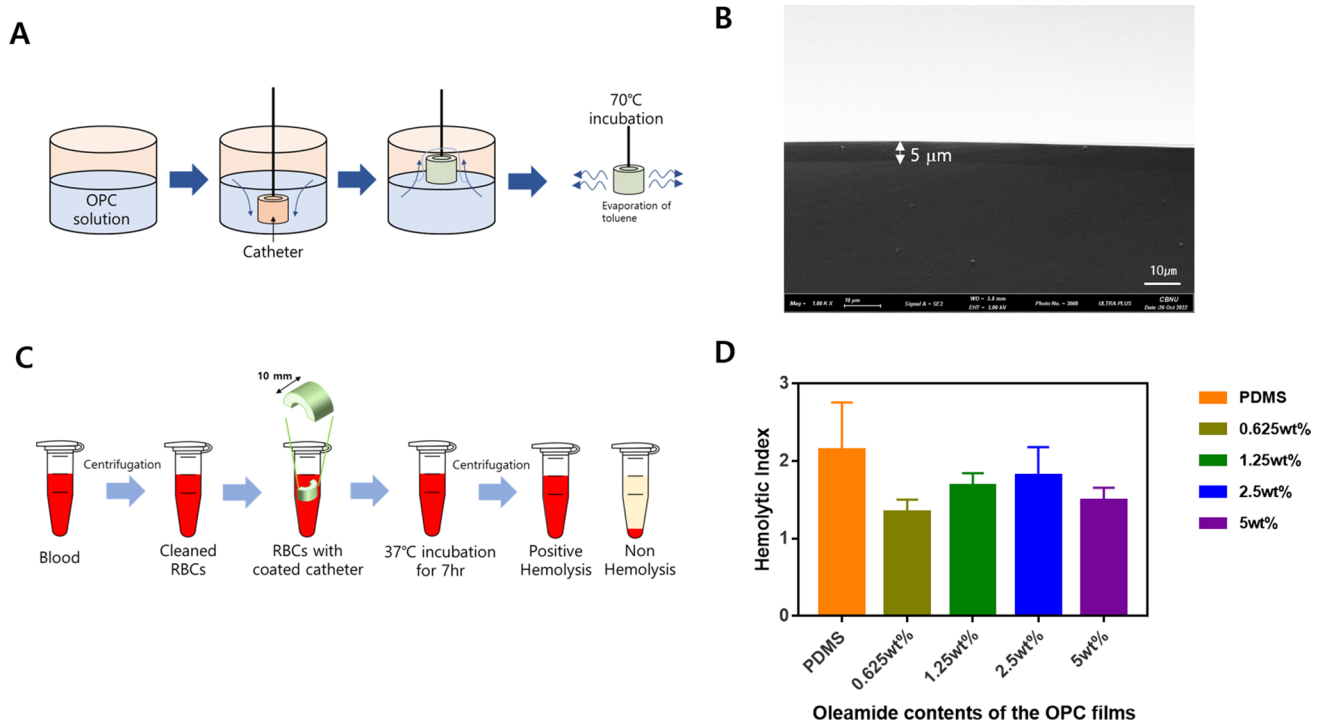
Fig. 4 **A** Simple dip-coating process for OPC-coated catheters. **B** FE-SEM (1000× magnification) image of cross section of OPC-coated catheters. Scale bar = 10 μm. **C** Hemolysis assay procedure for OPC-coated catheters. **D** Hemolytic index on PDMS, 5 wt%, 2.5 wt%, 1.25 wt%, and 0.625 wt% of OPC-coated catheters. The data were obtained from three independent experiments and analyzed by one-way ANOVA (Dunnett T3)

attached at the beginning is one of the factors that directly affects the survival and proliferation of bacteria in the biofilm (Carniello et al. 2018). The non-specific and reversible attachment of bacteria to surfaces synthesizes insoluble EPS, which develop into mature biofilms (Quinn et al. 2020). Because the EPS matrix protects bacteria from host immune responses, predators, and antimicrobial agents, one of the most effective ways to prevent biofilm formation is by inhibiting early bacterial attachment (Cheng et al. 2007). In this study, the initial suppression of the number of attached bacteria with increasing amounts of oleamide demonstrated anti-biofilm efficacy by significantly delaying the formation of a stable biofilm. However, OPC prevents biofouling and does not have antibacterial properties. The growth curves of bacteria cultured in OPC films and control bacteria show the same growth rate (Fig. S1). Therefore, OPC has no affect bacterial growth and does not cause drug resistance even at high concentrations. The superhydrophobic surfaces of PDMS can decrease bacterial adhesion by trapping a bubble layer on a rough surface with a low surface energy. However, this anti-biofouling property is not long lasting, as air bubbles dissolve in the medium solution (Hwang et al. 2018). The slippery surface of OPC has a stronger and longer-lasting anti-biofouling feature, preventing organisms from reaching the solid surface or deceiving

the sensing mechanism initiated for adhesive behavior (Amini et al. 2017).

The biocompatibility of the OPC-coated catheters was determined using a hemolysis assay. The US Food and Drug Administration (FDA) (ISO 10993) recommends that catheters be tested for hemolysis because RBC can negatively affect wound healing during surgical procedures. Hemolysis is the most common initial assessment of toxicity (Pietkiewicz et al. 2010). According to ASTM (Standard practice for assessment of hemolytic properties of materials, American Society of Testing and Materials Designation, ASTMF756-00), a non-hemolytic material has a hemolytic index of less than 2, and a slightly hemolytic material has a hemolytic index of between 2 and 5 (Laranjeira et al. 2016). Therefore, hemolytic index of OPC films from 1.35 ± 0.16 to 1.81 ± 0.37 are considered non-hemolytic. In this study, no significant difference in hemolysis was observed between the PDMS (control) and different oleamide concentrations. These results suggest that the biostability of the catheters coated with OPC was demonstrated by a low degree of hemolysis. Since biosafety cannot be guaranteed with hemolysis testing alone, biocompatibility and hazard risks must be confirmed its cytotoxicity, sensitization, and irritation through further studies. However, according to the research by Bertin et al. (Bertin et al. 2012), which investigated the hemolysis and

cytotoxicity of several fatty acid amides such as linoleamide and oleamide, cytotoxicity of oleamide begins at 100 μg/mL. In this study, the amount of oleamide in 1 cm catheter would be approximately 0.1 μg of 5 wt% OPC films, which will be highly difficult to show cytotoxicity. Based on the above several research results, the concentration of OPC used in this study is considered to be very unlikely to cause cytotoxicity and further toxicity in animals. Collectively, it can be considered to establish a disease animal model that requires the use of a urinary catheter and to confirm the toxicity and functionality of OPC by applying an OPC film to an in vivo model.

Conclusion

In this study, a PDMS coating film containing oleamide was synthesized and applied to catheters as a coating to evaluate its ability to inhibit biofilm formation and its biocompatibility. By inhibiting the initial bacterial adhesion, OPC prevented biofilm formation. FE-SEM and CLSM analyses confirmed that as the oleamide content increased, the ability to inhibit the surface adhesion of both *E. coli* and *S. aureus* also increased. In addition, biofilm formation was significantly suppressed in both *E. coli* and *S. aureus* at oleamide contents of 2.5% and 5wt%. Catheters were coated with a 5-μm-thick OPC layer using a simple dip-coating method, and biocompatibility was confirmed by hemolysis analysis. The results confirmed that the PDMS coating film containing oleamide exhibited biocompatibility that allows its application in biomedical devices and has antibacterial properties suitable for preventing infection by inhibiting initial bacterial adhesion in medical devices.

Author contributions JP, ES, and YSP designed research studies. JP and ES conducted the experiments. Y-HK, and J-YA revised the manuscript and corrected the figure results. KEL, and DHC performed data analysis. All the authors participated in manuscript preparation and approved the final manuscript.

Data availability The datasets generated during this study are available from the corresponding author on reasonable request.

Declarations

Conflict of interest Jiwon Park declares that she has no conflict of interest. Eunseok Seo declares that she has no conflict of interest. Yang-Hoon Kim declares that she has no conflict of interest. Ji-Young Ahn declares that she has no conflict of interest. Kyeong Eun Lee declares that she has no conflict of interest. Da Hyeon Choi declares that she has no conflict of interest. Yoon Shin Park declares that she has no conflict of interest.

Ethical approval This article does not contain any studies with human participants or animals performed by any of the authors.

References

Amini S, Kolle S, Petrone L, Ahanotu O, Sunny S, Sutanto CN, Hoon S, Cohen L, Weaver JC, Aizenberg J, Vogel N (1979) Ali Miserez † (2017) Preventing mussel adhesion using lubricant-infused materials. Science 357:668–673

Assefa M, Amare A (2022) Biofilm-associated multi-drug resistance in hospital-acquired infections: a review. Infect Drug Resist 15:5061–5068

Baidya S, Sharma S, Mishra SK, Kattel HP, Parajuli K, Sherchand JB (2021) Biofilm formation by pathogens causing ventilator-associated pneumonia at intensive care units in a tertiary care hospital: an armor for refuge. Biomed Res Int 2021:1–10

Bertin MJ, Zimba PV, Beauchesne KR, Huncik KM, Moeller PDR (2012) The contribution of fatty acid amides to prymnesium parvum carter toxicity. Harmful Algae 20:117–125

Briscoe BJ, Mustafaev V, Tabor D (1972) Lubrication of polythene by oleamide and stearamide. Wear 19:399–414

Carniello V, Peterson BW, van der Mei HC, Busscher HJ (2018) Physico-chemistry from initial bacterial adhesion to surface-programmed biofilm growth. Adv Colloid Interface Sci 261:1–14

Cheng G, Zhang Z, Chen S, Bryers JD, Jiang S (2007) Inhibition of bacterial adhesion and biofilm formation on zwitterionic surfaces. Biomaterials 28:4192–4199

D'Almeida RE, Molina RRDI, Viola CM, Luciardi MC, Nieto Peñalver C, Bardón A, Arena ME (2017) Comparison of seven structurally related coumarins on the inhibition of Quorum sensing of Pseudomonas aeruginosa and Chromobacterium violaceum. Bioorg Chem 73:37–42

Del Pozo JL (2018) Biofilm-related disease. Expert Rev Anti Infect Ther 16:51–65

Desrousseaux C, Sautou V, Descamps S, Traoré O (2013) Modification of the surfaces of medical devices to prevent microbial adhesion and biofilm formation. J Hosp Infect 85:87–93

Ding X, Yang C, Lim TP, Hsu LY, Engler AC, Hedrick JL, Yang YY (2012) Antibacterial and antifouling catheter coatings using surface grafted PEG-b-cationic polycarbonate diblock copolymers. Biomaterials 33:6593–6603

Dudeck MA, Horan TC, Peterson KD, Allen-Bridson K, Morrell G, Anttila A, Pollock DA, Edwards JR (2013) National Healthcare Safety Network report, data summary for 2011, device-associated module. Am J Infect Control 41:286–300

Getachew P, Getachew M, Joo J, Choi YS, Hwang DS, Hong YK (2016) The slip agents oleamide and erucamide reduce biofouling by marine benthic organisms (diatoms, biofilms and abalones). Toxicol Environ Health Sci 8:341–348

Greco I, Molchanova N, Holmedal E, Jenssen H, Hummel BD, Watts JL, Håkansson J, Hansen PR, Svenson J (2020) Correlation between hemolytic activity, cytotoxicity and systemic in vivo toxicity of synthetic antimicrobial peptides. Sci Rep 10:1–13

Harding JL, Reynolds MM (2014) Combating medical device fouling. Trends Biotechnol 32:140–146

Hrynyshyn A, Simões M, Borges A (2022) Biofilms in surgical site infections: recent advances and novel prevention and eradication strategies. Antibiotics 11:1–24

Hu X, Huang YY, Wang Y, Wang X, Hamblin MR (2018) Antimicrobial photodynamic therapy to control clinically relevant biofilm infections. Front Microbiol 9:1–24

Huitrón-Reséndiz S, Gombart L, Cravatt BF, Henriksen SJ (2001) Effect of oleamide on sleep and its relationship to blood pressure, body temperature, and locomotor activity in rats. Exp Neurol 172:235–243

Hwang GB, Page K, Patir A, Nair SP, Allan E, Parkin IP (2018) The anti-biofouling properties of superhydrophobic surfaces are short-lived. ACS Nano 12:6050–6058

Ishiguro A, Nishioka M, Morishige A, Kawano R, Kobayashi T, Fujinaga A, Takagi F, Kogo T, Morikawa Y, Okayama N, Mizuno H, Aihara M, Suehiro Y, Yamasaki T (2020) What is the best wavelength for the measurement of hemolysis index? Clin Chim Acta 510:15–20

Khatoon Z, McTiernan CD, Suuronen EJ, Mah T-F, Alarcon EI, Alarcon Bacterial EI (2018) Bacterial biofilm formation on implantable devices and approaches to its treatment and prevention. Heliyon 4:e01067

Kragh KN, Alhede M, Kvich L, Bjarnsholt T (2019) Into the well—a close look at the complex structures of a microtiter biofilm and the crystal violet assay. Biofilm 1:1–9

Laranjeira MS, Moço A, Ferreira J, Coimbra S, Costa E, Santos-Silva A, Ferreira PJ, Monteiro FJ (2016) Different hydroxyapatite magnetic nanoparticles for medical imaging: Its effects on hemostatic, hemolytic activity and cellular cytotoxicity. Colloids Surf B Biointerfaces 146:363–374

Larsen T, Fiehn NE (2017) Dental biofilm infections—an update. APMIS 125:376–384

Liu D, Huang Q, Gu W, Zeng XA (2022) A review of bacterial biofilm control by physical strategies. Crit Rev Food Sci Nutr 62:3453–3470

Lutufyo TE, Qin W, Chen X (2022) Central Line associated bloodstream infection in adult intensive care unit population—changes in epidemiology, diagnosis, prevention, and addition of new technologies. Adv Infect Dis 12:252–280

Mechmechani S, Khelissa S, Gharsallaoui A, El OK, Hamze M, Chihib NE (2022) Hurdle technology using encapsulated enzymes and essential oils to fight bacterial biofilms. Appl Microbiol Biotechnol 106:2311–2335

Nicolle LE (2014) Catheter associated urinary tract infections. Antimicrob Resist Infect Control 3:1–8

Pietkiewicz J, Zielińska K, Saczko J, Kulbacka J, Majkowski M, Wilk KA (2010) New approach to hydrophobic cyanine-type photosensitizer delivery using polymeric oil-cored nanocarriers: Hemolytic activity, in vitro cytotoxicity and localization in cancer cells. Eur J Pharm Sci 39:322–335

Quinn J, McFadden R, Chan C-W, Carson L (2020) Titanium for Orthopedic Applications: An Overview of Surface Modification to Improve Biocompatibility and Prevent Bacterial Biofilm Formation. iScience 23:101745

Ramasamy M, Lee J (2016) Recent nanotechnology approaches for prevention and treatment of biofilm-associated infections on medical devices. Biomed Res Int 2016:1–18

Rodrigues LR (2011) Inhibition of Bacterial Adhesion on Medical Devices. In: Linke D, Goldman A (eds) Bacterial adhesion: chemistry, biology and physics. Springer, Netherlands, Dordrecht, pp 351–367

Römling U, Balsalobre C (2012) Biofilm infections, their resilience to therapy and innovative treatment strategies. J Intern Med 272:541–561

Seo E, Seong MR, Lee JW, Lim H, Park J, Kim H, Hwang H, Lee D, Kim J, Kim GH, Hwang DS, Lee SJ (2020) Anti-Biofouling Features of Eco-Friendly Oleamide-PDMS Copolymers. ACS Omega 5:11515–11521

Srisang S, Nasongkla N (2019) Layer-by-layer dip coating of Foley urinary catheters by chlorhexidine-loaded micelles. J Drug Deliv Sci Technol 49:235–242

Tenke P, Kovacs B, Jäckel M, Nagy E (2006) The role of biofilm infection in urology. World J Urol 24:13–20

Torkzadeh H, Zodrow KR, Bridges WC, Cates EL (2021) Quantification and modeling of the response of surface biofilm growth to continuous low intensity UVC irradiation. Water Res 193:1–7

Trubenová B, Roizman D, Moter A, Rolff J, Regoes RR (2022) Population genetics, biofilm recalcitrance, and antibiotic resistance evolution. Trends Microbiol 30:841–852